

A procedure to specify the weighting matrices for an optimal load-frequency controller

Sílvio José Pinto Simões MARIANO^{1,*}, José Álvaro Nunes POMBO²,
Maria do Rosário Alves CALADO¹, Luís António Fialho Marcelino FERREIRA³

¹Department of Electromechanical Engineering, University of Beira Interior,
6201-001 Covilhã-PORTUGAL

e-mails: sm@ubi.pt, j_pombo@ipcb.pt, rc@ubi.pt, lmf@ist.utl.pt

²Department of Electrical Engineering, Polytechnic Institute of Castelo Branco,
6000-767 Castelo Branco-PORTUGAL

³Department of Electrical Engineering and Computers, Instituto Superior Técnico,
1049-001 Lisboa-PORTUGAL

Received: 16.03.2010

Abstract

The linear quadratic optimal regulator is one of the most powerful techniques for designing multivariable control systems. The performance of the system is specified in terms of a cost, which is the integral of a weighted quadratic function of the system state and control inputs, that is to be minimized by the optimal controller. The components of the state cost weighting matrix, Q , and the control cost weighting matrix, R , are ours to choose in mathematically specifying the way we wish the system to perform. Changing these matrices, we can modify the transient behavior of the closed-loop system. This paper addresses the stabilization and performance of the load-frequency controller by using the theory of the optimal control. A new technique, based on pole placement using optimal regulators, to overcome the difficulties of specifying weighting matrices Q and R is proposed. The design method employs successive shifting of either a real pole or a pair of complex conjugate poles at a time. The proposed technique builds Q and R in such a way that the system response also obeys conventional criteria for the system pole location. The effectiveness of the proposed method is illustrated by numerical examples.

Key Words: Power systems, load-frequency control, optimal control, weighting matrices

1. Introduction

Large-scale power systems are normally divided into control areas based on the principle of coherency. The coherent areas are interconnected through tie-lines, which are used for contractual energy exchange between areas and provide interarea support during abnormal operations.

*Corresponding author: Department of Electromechanical Engineering, University of Beira Interior, 6201-001 Covilhã-PORTUGAL

The objective of the automatic generation control (AGC) or load-frequency control (LFC) of a power system is to maintain the frequency of each area and tie-line power flow (in interconnected systems) within a specified tolerance. Many investigations in the area of AGC problems of interconnected systems have been reported in the past. The suggestions for dynamic modeling for AGC purposes that are followed in this paper are contained in [1-3], and are discussed thoroughly in [4]. A number of control schemes have been employed in the design of load-frequency controllers in order to achieve better dynamic performance, such as classical control [5,6], optimal control [7,8], and H-infinity methods with variable structure control [9]. Recently, load-frequency control as well the related voltage control have also been proposed, based on genetic algorithms [10,11], and the role of artificial intelligence in the reliability evaluation of electric power systems was addressed in [12]. In [13], combined intelligent techniques were used for autonomous AGC.

Among the aforementioned controllers, the most widely employed is the conventional proportional integral (PI) controller, due to its low cost and high reliability in operation. Although the PI controller is simple for implementation, it generally exhibits oscillatory frequency deviation responses.

The application of the optimal control theory to power systems has shown that an optimal load-frequency controller can improve the dynamic stability of a power system [14]. To achieve the desired response of a system without the expenditure of high control effort, optimal control is often employed. The optimal control law results from the minimization of a performance index, which is specified in terms of a cost defined by the integral of a weighted quadratic function of the system state and control inputs.

However, the application of optimal control theory has 2 fundamental (yet complementary) difficulties [15-17]: how to specify the matrices Q and R , and how to define the quality of the load-frequency controller. The problem of selecting weighting matrices Q and R has shown up in optimal control design [15-18]. To assign appropriate values for matrices Q and R in a systematic manner, avoiding the burdensome process of search by trial and error is a major concern, and it is the main point addressed in this paper.

The present paper develops a method to design a linear quadratic regulator that achieves the desired pole placement while satisfying the optimality. It follows the basic concept of shifting a single real pole or a pair of complex conjugate poles at a time. A weighting matrix is constructed in such a way that the desired pole location is achieved by the optimal feedback gain, which corresponds to the weighting matrix of the performance index. The feasibility of the pole shifting can be verified in each step of the design procedure, since this method utilizes the complete region of assignable closed-loop poles.

This paper is organized as follows: Section 2 presents the main results of the optimal control theory. Section 3 proposes an approach to perform the specification of the weighting matrices. Section 4 illustrates the proposed approach with numerical results. Section 5 concludes the paper.

2. Optimal control theory

To design a linear optimal control, a linearized model of the power system is sought. The linear time-invariant system model is described in state-space form as:

$$\begin{aligned} \dot{x}(t) &= Ax(t) + Bu(t) \\ y(t) &= Cx(t) \end{aligned} \quad x \in \mathfrak{R}^{n_x}, \quad u \in \mathfrak{R}^{n_u}, \quad y \in \mathfrak{R}^{n_y}, \quad (1)$$

where A and B are system matrices, x is the state vector, u is the control signal vector, y is the output vector, and n_x , n_u , and n_y are the number of state, control, and output variables, respectively.

Once the complete state x is available for feedback, it is possible to allocate the set of closed-loop system poles to an arbitrary position, by means of a suitable linear state feedback. Thus, the control law is [7]:

$$u(t) = -Kx(t), \quad (2)$$

where K is the feedback gain matrix, and the closed-loop system model can be rewritten as:

$$\dot{x} = [A - BK] x. \quad (3)$$

For the linear system described in Eq. (1), with a given controllable pair (A, B) , and if A is a nonsingular matrix, then the optimal control signal u that minimizes the performance index J , given by:

$$J = \int_0^{\infty} [x^T Q x + u^T R u] dt, \quad (4)$$

is a function of the present states of the system weighted by the components of a constant gain matrix K as:

$$u = -Kx = -R^{-1}B^T P x, \quad (5)$$

where Q and R are the weighting matrices, K is the feedback gain matrix, and P is the solution of the linear matrix Riccati equation:

$$A^T P + PA - PBR^{-1}B^T P + Q = 0. \quad (6)$$

The Riccati equation is the key to obtaining the optimal control. Once matrices Q and R are known, matrix P can be obtained by solving the Riccati equation. From Eq. (5), we get the optimal control vector u . However, the relationship between the weighting matrices and the closed-loop poles is not simple. The most common procedure for specifying matrix Q is searching by trial and error. Different matrices Q_i result in different gain matrices K_i , which in turn result in different dynamic performances for the closed-loop system. There are many possibilities to test by trial and error, which makes this procedure burdensome.

The present paper develops a method based on [19] for constructing a linear quadratic regulator that achieves the desired pole placement while satisfying the optimality. It follows the basic concept of shifting a single pole or a pair of complex conjugate poles at a time.

3. Project procedure

The proposed approach, based on optimal pole shift, assumes that the pair (A, B) in Eq. (1) is controllable, as was previously stated, and that the coefficient matrix A has distinct eigenvalues.

Consider now a specific mode of the system, which can be obtained from an appropriate linear transformation. The above assumption guarantees that the selected mode is controllable so that it can be chosen as a nonsingular matrix, M , according to:

$$MAM = \begin{bmatrix} A_{11} & \cdots & 0 \\ \vdots & \ddots & \vdots \\ 0 & \cdots & A_{nn} \end{bmatrix}, \quad (7)$$

and

$$M^{-1}BR^{-1}B^T (M^{-1})^T = \begin{bmatrix} V_{11} & \cdots & V_{1n} \\ \vdots & \ddots & \vdots \\ V_{1n}^T & \cdots & V_{nn} \end{bmatrix}, \quad (8)$$

where $A_{11} = \begin{bmatrix} \alpha & \beta \\ -\beta & \alpha \end{bmatrix}$ and $V_{11} = v_0 \begin{bmatrix} 1 & 0 \\ 0 & v \end{bmatrix}$,

with $v_0 > 0$, $0 \leq v \leq 1$.

The first 2 columns of the transformation matrix, A_{11} , result from the real part and the imaginary part of the eigenvectors of A , corresponding to the eigenvalues $\alpha \pm j\beta$. Let this transformation matrix be M_1 , with the other columns of the transformation matrix assumed to be irrelevant.

Matrix V_{11} is symmetric and positive semidefinite in general. Thus, it can be diagonalized and the arbitrary ordering of the eigenvalues is possible with an orthogonal transformation matrix, appending the identity matrix to this orthogonal matrix to form a block diagonal matrix with the size of A . Let us denote this matrix as M_2 , and then the transformation matrix M is $M = M_1 M_2$.

The selection of weighting matrix R is arbitrary, and it is used as a scaling factor for the input channels. Nevertheless, scaling R for the inputs of the system has no effect, since it will only result in same amount of scaling on Q .

The weighting matrix Q is to be constructed according to the pole assignment; let Q_{11} be a positive semidefinite matrix with the same size as A_{11} , and set a weighting matrix Q that satisfies:

$$Q = (M^{-1})^T \begin{bmatrix} Q_{11}/v_0 & 0 \\ 0 & 0 \end{bmatrix} M^{-1} \tag{9}$$

The eigenvalues of A_{11} can then be shifted while keeping all other eigenvalues of A unchanged.

3.1. Pole shifting: weighting matrices specification

When a real pole is to be shifted, the matrices A_{11} , V_{11} , and Q_{11} reduce to scalar. In this case, the assignable region of optimal closed-loop poles is readily determined. It turns out that a real pole, either stable or unstable, can only be shifted along the real axis within the left half of the complex plane, and that the absolute value of the closed-loop pole is larger than that of the open-loop pole and can be given by Eq. (9), with $Q_{11} = (\alpha_d)^2 - (\alpha)^2$.

When a complex conjugate pole is to be shifted, the matrices A_{11} , V_{11} , and Q_{11} are 2×2 matrices. In this case, the Hamilton matrix assumes the form:

$$H = \begin{bmatrix} A_{11} & V_{11} \\ -Q_{11} & -A_{11}^T \end{bmatrix} \tag{10}$$

and is associated with the regulator problem of the second-order system. Let the entries of Q_{11} be described as:

$$Q_{11} = \begin{bmatrix} q_1 & q_2 \\ q_3 & q_4 \end{bmatrix} \tag{11}$$

The characteristic equation of H then has the form:

$$s^4 + C_2 s^2 + C_0 = 0. \tag{12}$$

The coefficients C_2 and C_0 turn out to be:

$$C_2 = 2(\beta^2 - \alpha^2) - \overline{C}_2, \tag{13}$$

$$C_0 = (\beta^2 + \alpha^2)^2 - \overline{C}_0, \tag{14}$$

where:

$$\overline{C}_2 = q_1 + v q_3, \quad (15)$$

$$\overline{C}_0 = (\alpha^2 + v \beta^2) q_1 + 2(1-v) \alpha \beta q_2 + (v \alpha^2 + \beta^2) q_3 + v (q_1 q_3 - q_2^2). \quad (16)$$

Here, \overline{C}_2 and \overline{C}_0 represent the terms that depend on weighting matrix Q_{11} .

Let weighting matrix Q_{11} correspond to the optimal closed-loop poles $\alpha_d \pm j\beta_d$, and then the coefficients C_2 and C_0 are described by:

$$C_2 = 2(\beta_d^2 - \alpha_d^2), \quad (17)$$

$$C_0 = (\beta_d^2 + \alpha_d^2)^2. \quad (18)$$

Assume that the 2×2 weighting matrix, Q_{11} , is restricted to be singular. In this case, it can be described in dyadic form as:

$$Q_{11} = \begin{bmatrix} \rho \cos^2(\theta) & \rho \sin(\theta) \cos(\theta) \\ \rho \sin(\theta) \cos(\theta) & \rho \sin^2(\theta) \end{bmatrix} \quad (19)$$

where $\rho > 0$ and $0 \leq \theta < \pi$.

Now parameters \overline{C}_2 and \overline{C}_0 can be expressed in terms of ρ and θ as:

$$\overline{C}_2 = \frac{\rho}{2} ((1+v) + (1-v) \cos(2\theta)), \quad (20)$$

$$\overline{C}_0 = \frac{\rho}{2} (\alpha^2 - \beta^2) ((1+v) + (1-v) \cos(2\theta + \phi)), \quad (21)$$

where ϕ satisfies:

$$\sin(\phi) = \frac{-2\alpha\beta}{\alpha^2 + \beta^2}, \quad \cos(\phi) = \frac{\alpha^2 - \beta^2}{\alpha^2 + \beta^2}. \quad (22)$$

Resolving the system given by Eqs. (20) and (21) for ρ , and θ Q_{11} is obtained through Eq. (19). Substituting in Eq. (9), the eigenvalues of A_{11} can be shifted while keeping all other eigenvalues of A unchanged. To shift all poles together, the weighting matrix Q and the corresponding optimal feedback gain matrix K are, respectively,

$$Q = \sum_{i=0}^{n_x} Q_i \quad \text{and} \quad K = \sum_{i=0}^{n_x} K_i. \quad (23)$$

3.2. Algorithm to specify the weighting matrices

The adopted method to perform the pole shifting is now summarized in the following steps.

Algorithm

Step 1 - Calculate the feedback closed-loop eigenvalues and the eigenvectors corresponding to gain matrix K_i .

Step 2 - Choose a transformation matrix M so that the partitioned matrices A_{11} and V_{11} represent either a real pole or a pair of complex conjugate poles to be shifted.

Step 3 - Find a weighting matrix Q_{11} with which the desired pole positioning is accomplished.

Step 4 - Calculate the weighting matrix Q and the corresponding optimal feedback gain K for the whole system, and then form a closed-loop system with K .

Step 5 - Go to Step 1 while there are remaining poles to be shifted.

Step 6 - Calculate the sum of the matrices Q and K in each step to obtain the weighting and optimal feedback gain matrices, which achieve the desired pole location.

An illustration of the proposed algorithm is shown in the flowchart of Figure 1.

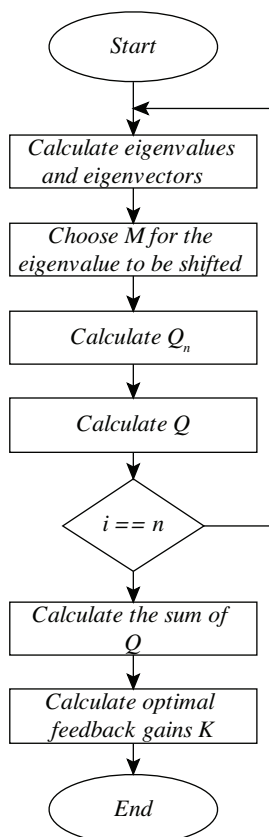


Figure 1. Flowchart of the proposed algorithm.

4. Results and discussion

To illustrate the proposed algorithm, a system of 4 different interconnected areas were considered: an area with hydropower plants (area 1); 2 areas with fossil power plants, 1 with a nonreheat steam system configuration (area 2) and the other with a tandem compound, single reheat steam system configuration (area 3); and the last area considered to have infinite kinetic energy (area 4).

This case study can be compared to an interconnection of the power systems of individual utilities. Each company operates independently within its own jurisdiction, but there are contractual agreements about intercompany exchanges of power through the tie-lines and other agreements about operating procedures to maintain system frequency. The adjustment of the command increment, ΔP_{r_i} , is done automatically and according to the contractual agreements.

We combined the 4-area system and a model was obtained. This model is shown in Figure 2, using a

block diagram representation, and the system is defined by the symbols and parameters shown in the List of Symbols, where $K_p = 1/D_i$ and $T_p = 2H_i/D_i$.

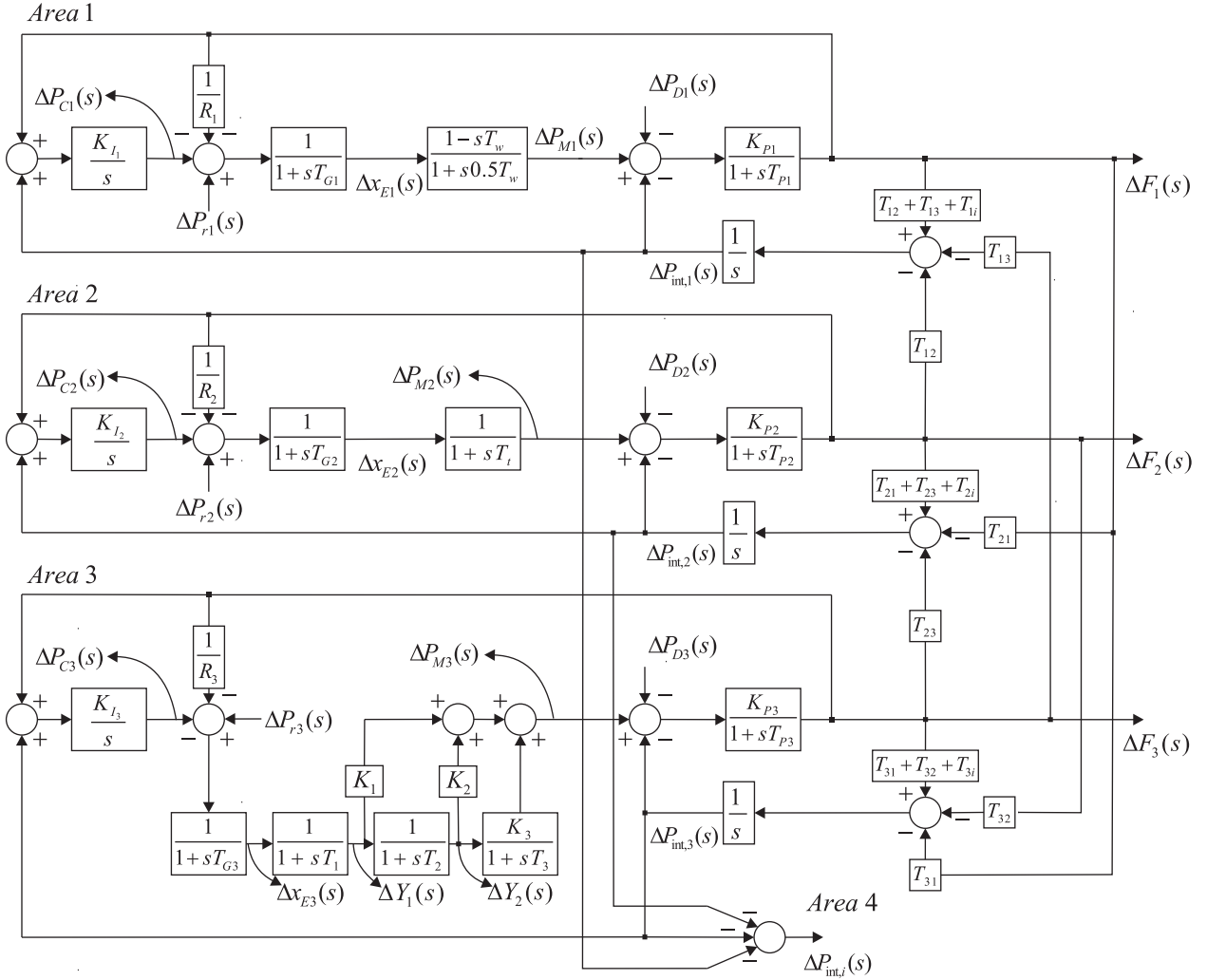


Figure 2. Block diagram of 4-area perturbation model.

As a result, a linear model of the system, in state-space form, is obtained:

$$\dot{x} = Ax + Bu + \Gamma \Delta P_D. \tag{24}$$

The state vector is defined as:

$$x = \begin{bmatrix} \Delta f_1 & \Delta f_2 & \Delta f_3 & \vdots & \Delta p_{int,1} & \Delta p_{int,2} & \Delta p_{int,3} & \vdots \\ \Delta p_{M_1} & \Delta p_{M_2} & \Delta p_{x_1} & \Delta p_{x_2} & \Delta p_{M_3} & \vdots & & \\ \Delta x_{E_1} & \Delta x_{E_2} & \Delta x_{E_3} & \vdots & \Delta p_{C_1} & \Delta p_{C_2} & \Delta p_{C_3} \end{bmatrix}$$

The control vector and incremental load demand change vector are defined, respectively, as:

$$u = \begin{bmatrix} \Delta p_{r_1} \\ \Delta p_{r_2} \\ \Delta p_{r_3} \end{bmatrix} \text{ and } \Delta P_D = \begin{bmatrix} \Delta p_{D_1} \\ \Delta p_{D_2} \\ \Delta p_{D_3} \end{bmatrix}.$$

Substituting the definition of the states and the control into the 17 differential equations that define the 4-area system, we can obtain, respectively, the state matrix A , the control matrix B , and the disturbance matrix Γ , resulting in a completely controllable and observable system.

$$A = \begin{bmatrix} \frac{-1}{T_{P1}} & 0 & 0 & \frac{-K_{P1}}{T_{P1}} & 0 & 0 & \frac{K_{P1}}{T_{P1}} & 0 & 0 & 0 & 0 & 0 & 0 & 0 & 0 & 0 & 0 \\ 0 & \frac{-1}{T_{P2}} & 0 & 0 & \frac{-K_{P2}}{T_{P2}} & 0 & 0 & \frac{K_{P2}}{T_{P2}} & 0 & 0 & 0 & 0 & 0 & 0 & 0 & 0 & 0 \\ 0 & 0 & \frac{-1}{T_{P3}} & 0 & 0 & \frac{-K_{P3}}{T_{P3}} & 0 & 0 & 0 & 0 & \frac{K_{P3}}{T_{P3}} & 0 & 0 & 0 & 0 & 0 & 0 \\ T_{12} + T_{13} + T_{1i} & -T_{12} & -T_{13} & 0 & 0 & 0 & 0 & 0 & 0 & 0 & 0 & 0 & 0 & 0 & 0 & 0 & 0 \\ -T_{21} & T_{21} + T_{23} + T_{2i} & -T_{23} & 0 & 0 & 0 & 0 & 0 & 0 & 0 & 0 & 0 & 0 & 0 & 0 & 0 & 0 \\ -T_{31} & -T_{32} & T_{31} + T_{32} + T_{3i} & 0 & 0 & 0 & 0 & 0 & 0 & 0 & 0 & 0 & 0 & 0 & 0 & 0 & 0 \\ \frac{1}{0.5R_1T_{G1}} & 0 & 0 & 0 & 0 & 0 & \frac{-1}{0.5T_W} & 0 & 0 & 0 & 0 & \frac{T_{G1} + T_W}{0.5T_{G1}T_W} & 0 & 0 & \frac{-1}{0.5T_{G1}} & 0 & 0 \\ 0 & 0 & 0 & 0 & 0 & 0 & 0 & \frac{-1}{T_i} & 0 & 0 & 0 & 0 & \frac{1}{T_i} & 0 & 0 & 0 & 0 \\ 0 & 0 & 0 & 0 & 0 & 0 & 0 & 0 & \frac{-1}{T_1} & 0 & 0 & 0 & 0 & \frac{1}{T_1} & 0 & 0 & 0 \\ 0 & 0 & 0 & 0 & 0 & 0 & 0 & 0 & \frac{1}{T_2} & \frac{-1}{T_2} & 0 & 0 & 0 & 0 & 0 & 0 & 0 \\ 0 & 0 & 0 & 0 & 0 & 0 & 0 & 0 & \frac{K_1}{T_3} - \frac{K_1}{T_1} - \frac{K_2}{T_2} & \frac{K_2}{T_3} - \frac{K_3}{T_3} - \frac{K_2}{T_2} & \frac{-1}{T_3} & 0 & 0 & \frac{K_1}{T_1} & 0 & 0 & 0 \\ \frac{-1}{R_1T_{G1}} & 0 & 0 & 0 & 0 & 0 & 0 & 0 & 0 & 0 & 0 & 0 & \frac{-1}{T_{G1}} & 0 & 0 & \frac{1}{T_{G1}} & 0 & 0 \\ 0 & \frac{-1}{R_2T_{G2}} & 0 & 0 & 0 & 0 & 0 & 0 & 0 & 0 & 0 & 0 & 0 & \frac{-1}{T_{G2}} & 0 & 0 & \frac{1}{T_{G2}} & 0 \\ 0 & 0 & \frac{-1}{R_3T_{G3}} & 0 & 0 & 0 & 0 & 0 & 0 & 0 & 0 & 0 & 0 & 0 & \frac{1}{T_{G3}} & 0 & 0 & \frac{1}{T_{G3}} \\ 0 & 0 & 0 & -K_{i1} & 0 & 0 & 0 & 0 & 0 & 0 & 0 & 0 & 0 & 0 & 0 & 0 & 0 & 0 \\ 0 & 0 & 0 & 0 & -K_{i2} & 0 & 0 & 0 & 0 & 0 & 0 & 0 & 0 & 0 & 0 & 0 & 0 & 0 \\ 0 & 0 & 0 & 0 & 0 & -K_{i3} & 0 & 0 & 0 & 0 & 0 & 0 & 0 & 0 & 0 & 0 & 0 & 0 \end{bmatrix}$$

$$B' = \begin{bmatrix} 0 & 0 & 0 & 0 & 0 & 0 & \frac{-1}{0.5T_{G1}} & 0 & 0 & 0 & 0 & \frac{1}{T_{G1}} & 0 & 0 & 0 & 0 & 0 & 0 \\ 0 & 0 & 0 & 0 & 0 & 0 & 0 & 0 & 0 & 0 & 0 & 0 & \frac{1}{T_{G2}} & 0 & 0 & 0 & 0 & 0 \\ 0 & 0 & 0 & 0 & 0 & 0 & 0 & 0 & 0 & 0 & 0 & 0 & 0 & \frac{1}{T_{G3}} & 0 & 0 & 0 & 0 \end{bmatrix},$$

$$\Gamma' = \begin{bmatrix} \frac{-K_{P1}}{T_{P1}} & 0 & 0 & 0 & 0 & 0 & 0 & 0 & 0 & 0 & 0 & 0 & 0 & 0 & 0 & 0 & 0 & 0 \\ 0 & \frac{-K_{P2}}{T_{P2}} & 0 & 0 & 0 & 0 & 0 & 0 & 0 & 0 & 0 & 0 & 0 & 0 & 0 & 0 & 0 & 0 \\ 0 & 0 & \frac{-K_{P3}}{T_{P3}} & 0 & 0 & 0 & 0 & 0 & 0 & 0 & 0 & 0 & 0 & 0 & 0 & 0 & 0 & 0 \end{bmatrix}.$$

Applying the proposed algorithm defined in Section 3.2, for the parameters given in the List of Symbols, we can specify the weighting matrix Q , while R is specified as the identity matrix since, as stated above, it is only used as a scaling factor on the input channels to penalize for large control effort. Gain matrix K , for convenience and with the aim of generating more understandable results, is subdivided into 5 submatrices,

$$K = \begin{bmatrix} K_{SP} & : & K_{INT} & : & K_T & : & K_R & : & K_{CI} \end{bmatrix},$$

corresponding to the feedback gains of the state variable and respectively defining K_{SP} , the feedback gains for the incremental frequency deviation; K_{INT} , the feedback gains for the net incremental real power exported

from area i ; K_T , the feedback gains for the governor; K_R , the feedback gains for the regulator; and K_{CI} , the feedback gains for the integral control.

The weighting matrix Q and the gain matrix K are, respectively,

$$Q = \begin{bmatrix} 7.3 & 5.8 & -1.1 & 25.4 & 12.3 & 6.7 & 3.4 & 1.1 & 2.4 & 87.3 & -13.4 & 13.2 & 1.3 & 0.7 & 1.1 & -20.2 & -12.3 \\ 5.8 & 20.3 & 8.3 & 24.5 & 67.3 & 20.2 & 1.4 & 7.1 & 0.7 & 12.1 & -6.5 & 2.1 & 7.9 & 1.2 & 2.6 & -32.4 & -31.3 \\ -1.1 & 8.3 & 120 & 16.3 & 7.7 & 3.31 & -0.5 & 1.2 & -0.4 & 2.9 & -8.6 & 23.4 & -0.2 & -0.41 & 1.8 & -21.8 & -67.3 \\ 25.4 & 24.5 & 16.3 & 12.1 & 1.5 & 6.7 & -1.2 & 17.8 & -0.1 & 1.7 & 12.8 & -1.2 & 28.1 & 10.1 & 2 & -9.1 & -13.1 \\ 12.3 & 67.3 & 7.7 & 1.5 & 66.1 & 23.4 & 28.9 & 12.5 & 0.1 & -1.8 & 1.7 & 12.6 & 34.2 & 15.2 & 13.6 & 12.9 & -34.7 \\ 6.7 & 20.2 & 3.31 & 6.7 & 23.4 & 71.2 & 5.8 & 11.9 & 2.1 & -9.8 & -15.6 & 14.2 & 19.8 & 21.8 & 21.1 & -9.4 & -18.9 \\ 3.4 & 1.4 & -0.5 & -1.2 & 28.9 & 5.8 & 43.4 & 25.4 & 5.8 & 60.5 & -11.9 & 5.4 & 4.7 & 1.4 & -23.5 & 22.1 & 16.7 \\ 1.1 & 7.1 & 1.2 & 17.8 & 12.5 & 11.9 & 25.4 & 18.4 & 0.8 & 1.2 & 0.1 & 19.5 & 2.2 & 82.9 & 0.1 & -15.9 & 17.1 \\ 2.4 & 0.7 & -0.4 & -0.1 & 0.1 & 2.1 & 5.8 & 0.8 & 5.4 & 14.7 & 53.5 & -35.1 & 4.1 & 21.1 & -15.6 & -89.4 & -46.5 \\ 87.3 & 12.1 & 2.9 & 1.7 & -1.8 & -9.8 & 60.5 & 1.2 & 14.7 & 67.9 & -11.9 & 5.4 & 4.7 & -36.1 & 13.5 & -18.6 & 13.9 \\ -13.4 & -6.5 & -8.6 & 12.8 & 1.7 & -15.6 & -11.9 & 0.1 & 53.5 & -11.9 & 78.5 & -35.1 & 0.8 & 2.1 & -54.6 & -9.8 & -46.9 \\ 13.2 & 2.1 & 23.4 & -1.2 & 12.6 & 14.2 & 5.4 & 19.5 & -35.1 & 5.4 & -35.1 & 123 & 34.6 & 18.1 & 15.3 & -20.5 & 132 \\ 1.3 & 7.9 & -0.2 & 28.1 & 34.2 & 19.8 & 4.7 & 2.2 & 4.1 & 4.7 & 0.8 & 34.6 & 17.9 & 98.2 & 17.9 & -45.8 & 48.3 \\ 0.7 & 1.2 & -0.41 & 10.1 & 15.2 & 21.8 & 1.4 & 82.9 & 21.1 & -36.1 & 2.1 & 18.1 & 98.2 & 1.1 & 14.8 & -76.3 & 4.8 \\ 1.1 & 2.6 & 1.8 & 2 & 13.6 & 21.1 & -23.5 & 0.1 & -15.6 & 13.5 & -54.6 & 15.3 & 17.9 & 14.8 & 28.9 & -35.1 & 52.8 \\ -20.2 & -32.4 & -21.8 & -9.1 & 12.9 & -9.4 & 22.1 & -15.9 & -89.4 & -18.6 & -9.8 & -20.5 & -45.8 & -76.3 & -35.1 & 67.7 & 43.4 \\ -12.3 & -31.3 & -67.3 & -13.1 & -34.7 & -18.9 & 16.7 & 17.1 & -46.5 & 13.9 & -46.9 & 132 & 48.3 & 4.8 & 52.8 & 43.4 & 86.4 \end{bmatrix}$$

and

$$K_{SP} = \begin{bmatrix} 0.49 & 0.18 & -1.01 \\ 0.44 & 1.9 & 0.82 \\ 1.25 & 0.94 & 14.7 \end{bmatrix}, \quad K_{INT} = \begin{bmatrix} -0.37 & 0.23 & -0.18 \\ 1.48 & 2.34 & 0.78 \\ 5.83 & 6.99 & 4.77 \end{bmatrix},$$

$$K_T = \begin{bmatrix} 0.23 & 0.11 & 0.25 & 2.67 & -1.10 \\ 0.07 & 2.01 & -0.35 & -1.08 & 1.67 \\ 0.51 & 0.56 & -2.62 & -13.34 & 16.35 \end{bmatrix},$$

$$K_R = \begin{bmatrix} 0.96 & 0.03 & -0.03 \\ 0.88 & 0.33 & 0.16 \\ 1.39 & 0.26 & 2.13 \end{bmatrix}, \quad K_{CI} = \begin{bmatrix} -0.27 & 0.09 & 2.72 \\ -0.61 & -3.28 & -2.16 \\ -4.63 & -7.05 & -34.4 \end{bmatrix}.$$

Since the closed-loop system eigenvalues can be arbitrarily placed anywhere in the left side of the complex plane, from an optimization point of view, the amount of improvement in system transients can be as large as we want. Optimal control has, when compared with other methods, especially effective results in damping fast and oscillatory responses of the state variables. However, the larger the distance of the pole's location to the imaginary axis is, the more demanding the physical control signal output will be. Thus, a careful study must be performed before the pole location assignment, in order to keep the control effort similar to that required by the classical proportional integral controller.

A 10% step-load increase ($\Delta P_D = 0.1$ pu MW) was applied to area 1 to illustrate the time evolution of frequency deviations Δf_1 , Δf_2 , and Δf_3 ; the tie-line power deviations $\Delta P_{int,1}$, $\Delta P_{int,2}$, $\Delta P_{int,3}$, and $\Delta P_{int,\infty}$; and the optimal output control signal. Figures 3 and 4 illustrate, respectively, the time evolution of the system frequency deviations for each area with classical control and with optimal control. Figures 5 and 6 illustrate the time evolution of the tie-line power deviation for each area with classical control and with optimal control, respectively.

From these results, along with many others obtained but not discussed herein, some conclusions can be made. First, the performance of the system with optimal state feedback controller (Figures 4 and 6) exhibits better damping than with the conventional control (Figures 3 and 5); optimal controllers are especially effective in damping fast the oscillatory frequency deviations and tie-line load. Second, considering the specified system pole location, the increase of the stability margin of optimal solution, as can be seen in Figures 4 and 6, was expected.

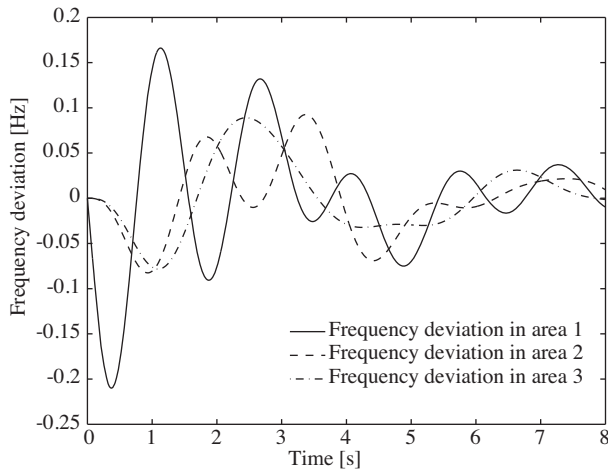


Figure 3. Step response of system frequency deviations with classical control.

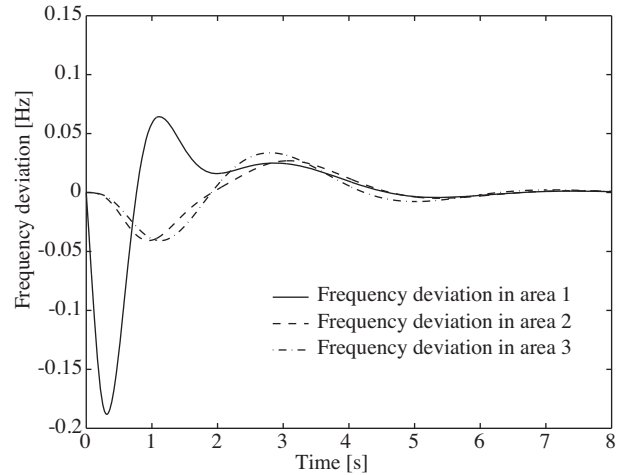


Figure 4. Step response of system frequency deviations with optimal control.

A significant improvement in system transients of the tie-line power deviations for the same steady-state performance was obtained, as shown in Figures 5 and 6. It can also be seen that, since area 4 is considered to have infinite kinetic energy, it is the area that contributes most to satisfying the step-load increase in area 1. Thus, the interconnection is effective in delivering power to control area 1, especially with optimal control.

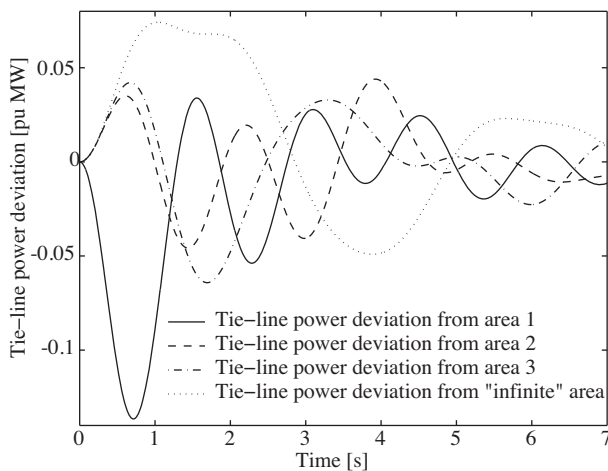


Figure 5. Step response of system tie-line power deviation with classical control.

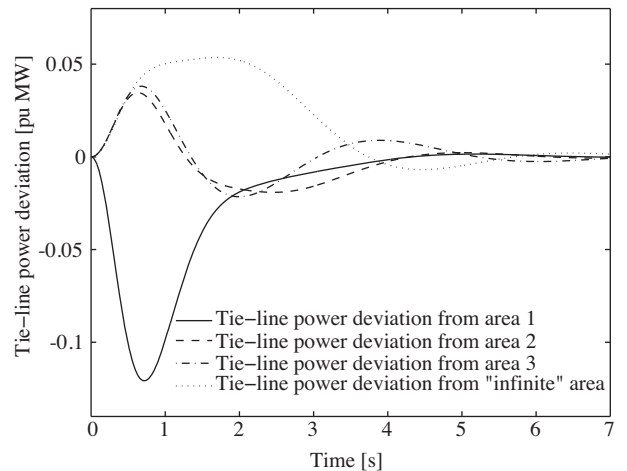


Figure 6. Step response of system tie-line power deviation with optimal control.

It can also be noted that the solution presented here does not require the elimination of conventional integral control. Therefore, the tie-line power deviations of each area are back to normal, or the basic principles of pool operation (scheduled interchanges of tie-line power are maintained and each area absorbs its own load changes) are satisfied.

Figures 7-9 illustrate the obtained output control signals u for area 1, area 2, and area 3, respectively. It is seen that, for all output control signals, classical control lead to results physically more demanding than those from the optimal controller. The optimal output control signals in area 2 and area 3 also have a high value of initial slope, while classical control exhibits zero initial slope. Only in area 1 does the output control signal exhibit high initial slope with classical control, because the step load is applied in this area. Note that the final value of the output control signal in area 1 (Figure 7) is equal to the step-load increase, forcing area 1 to absorb its own load changes. In the other areas, the final values of the output control signals are zero, despite the important contribution to load change in the transient responses.

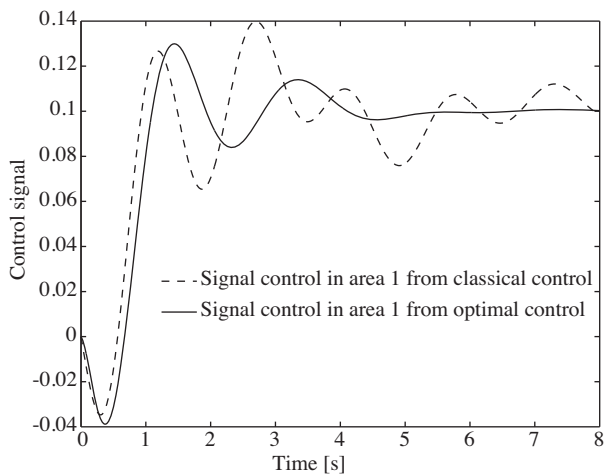


Figure 7. Signal control in area 1.

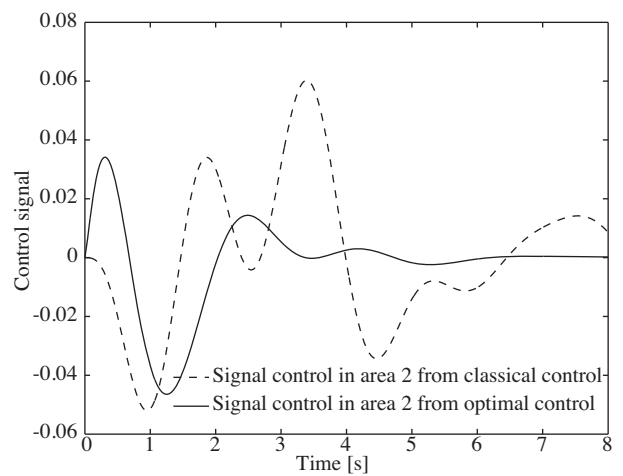


Figure 8. Signal control in area 2.

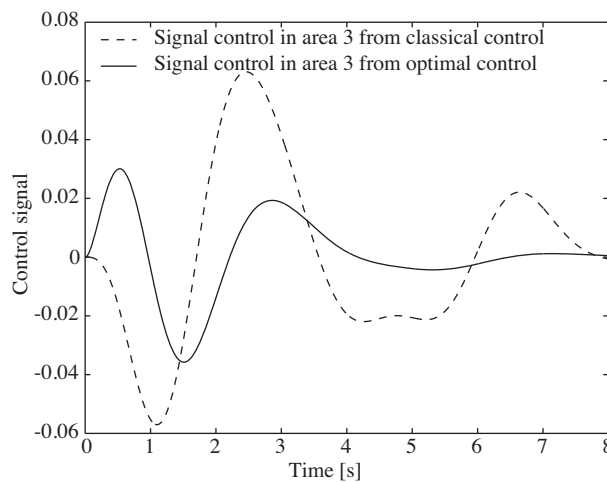


Figure 9. Signal control in area 3.

5. Conclusions

The paper has presented an optimal controller solution of the load-frequency control problem of large interconnected power systems (a multiarea electric energy system). A new technique that allows the specification of weighting matrices Q and R , avoiding the burdensome task of trial and error, was described and applied. The proposed method builds Q and R in such a way that the systems response also obeys conventional criteria for the system pole location while satisfying the optimality, following the basic concept of shifting a single real pole or a pair of complex conjugate poles at a time. An algorithm for the proposed methodology was clearly described, and a practical realization of this optimal approach for a 4-area interconnected power system was carried out and compared with the classical control. The obtained illustration results showed that the optimal controller yields results that are robust, with a highly improved performance.

List of symbols

Δf_i	incremental frequency deviation in area i
ΔP_{M_i}	incremental generated real power (mechanical power) deviation in area i
$\Delta P_{int,i}$	net incremental real power exported from area i
H_i	inertia constant ($H_1 = 0.06$, $H_2 = 0.1$, and $H_3 = 0.16$ s)
T_{G_i}	governor time constant ($T_{G_1} = 0.08$, $T_{G_2} = 0.1$, and $T_{G_3} = 0.2$ s)
R_i	drop constant ($R_1 = 5$, $R_2 = 2.5$, and $R_3 = 2.6$ Hz/pu MW)
T_{ij}	transmission constant (considered equal for all interconnections, $T_{ij} = 0.5$ pu MW/Hz)
T_w	hydro turbine time constant ($T_w = 0.1$ s)
T_T	nonreheat turbine time constant ($T_T = 0.3$ s)
D_i	system damping ($D_1 = D_2 = D_3 = 0.01$ pu MW/Hz)
$\Delta P_{x1}, \Delta P_{x2}$	incremental fraction generated power in tandem compound, single reheat turbine
T_1, T_2, T_3	tandem compound and single reheat turbine time constants ($T_1 = 0.2$, $T_2 = 6$, and $T_3 = 0.4$ s)
K_1, K_2, K_3	tandem compound and single reheat cylinder fractions ($K_1 = 0.3$, $K_2 = 0.4$, and $K_3 = 0.3$)

References

- [1] IEEE PES Committee Report, "Dynamic models for steam and hydro turbines in power system studies", IEEE Transactions on Power Apparatus and Systems, Vol. PAS-92, pp. 1904-1915, 1973.
- [2] IEEE PES Working Group, "Dynamic models for fossil fueled steam units in power system studies", IEEE Transactions on Power Systems, Vol. PWRS-6, pp. 753-761, 1991.
- [3] IEEE PES Working Group, "Hydraulic turbine and turbine control models for system dynamic studies", IEEE Transactions on Power Systems, Vol. PWRS-7, pp. 167-179, 1992.
- [4] P. Kundur, Power System Stability and Control, New York, McGraw-Hill, 1994.
- [5] J. Nanda, B. Kaul, "Automatic generation control of an interconnected power system", IEE Proceedings, Vol. 125, pp. 385-390, 1978.
- [6] O.I. Elgerd, C.E. Fosha, Jr., "Optimum megawatt-frequency control of multiarea electric energy systems", IEEE Transactions on Power Apparatus and Systems, Vol. PAS-89, pp. 556-563, 1970.
- [7] C.E. Fosha, Jr., O.I. Elgerd, "The megawatt-frequency control problem: a new approach via optimal control theory", IEEE Transactions on Power Apparatus and Systems, Vol. PAS-89, pp. 563-577, 1970.

- [8] F. Liu, Y.H. Song, J. Ma, S. Mai, Q. Lu, "Optimal load-frequency control in restructured power systems", IEE Proceedings Generation, Transmission and Distribution, Vol. 150, pp. 87-95, 2003.
- [9] H. Çimen, "Decentralised H_{∞} load frequency controller design based on SSVs", Turkish Journal of Electrical Engineering and Computer Sciences, Vol. 8, pp. 43-53, 2000.
- [10] G. Panda, S. Panda, C. Ardil, "Automatic generation control of multi-area electric energy systems using modified GA", International Journal of Energy and Power Engineering, Vol. 3, pp. 419-427, 2010.
- [11] D. Joshi, K.S. Sandhu, M.K. Soni, "Voltage control of self-excited induction generator using genetic algorithm", Turkish Journal of Electrical Engineering and Computer Sciences, Vol. 17, pp. 87-97, 2009.
- [12] C. Singh, L. Wang, "Role of artificial intelligence in the reliability evaluation of electric power systems", Turkish Journal of Electrical Engineering and Computer Sciences, Vol. 16, pp. 189-200, 2008.
- [13] Y.L. Karnavas, D.P. Papadopoulos, "AGC for autonomous power system using combined intelligent techniques", Electric Power System Research, Vol. 62, pp. 225-239, 2002.
- [14] S.J.P.S. Mariano, J.A.N. Pombo, M.R.A. Calado, L.A.F.M. Ferreira, "Optimal output control: load frequency control of a large power system", International Conference on Power Engineering, Energy and Electrical Drives, pp. 369-374, 2009.
- [15] W.S. Levine, M. Athans, "On the determination of the optimal constant output feedback gains for linear multivariable systems", IEEE Transactions on Automation Control, Vol. AC-15, pp. 44-48, 1970.
- [16] M. Calovic, "Linear regulator design for a load and frequency control", IEEE Transactions on Power Apparatus and Systems, Vol. PAS-91, pp.2271-2285, 1972.
- [17] J.A. Rovnak, R. Corlis, "Dynamic matrix based control of fossil power plants", IEEE Transactions on Energy Conversion, Vol. 6, pp. 320-326, June 1991.
- [18] S.J.P.S. Mariano, L.A.F.M. Ferreira, "A procedure to specify Q and R for an optimal voltage regulator", Proceedings of the IASTED International Conference, Las Vegas, USA, 1999.
- [19] T. Fujinaka, S Omatu, "Pole placement using optimal regulators", Transactions on IEE Japan, Vol. 121-C, pp. 240-245, 2001.